M. A. Krivoglaz for his careful review of the manuscript.

### References

AQUA, E. N. & WAGNER, C. N. J. (1964). *Philos. Mag.* **9**, 565-589.
DESPUJOLS, J. & WARREN, B. E. (1958). *J. Appl. Phys.* **29**, 195-199.
HOUSKA, C. R. & SMITH, T. (1981). *J. Appl. Phys.* **52**, 748-754.
KRIVOGLAZ, M. A., MARTYNENKO, O. V. & RYABOSHOPKA, K. P. (1983). *Phys. Met. Metall.* **55**, 1-12.
MCKEEHAN, M. & WARREN, B. E. (1953). *J. Appl. Phys.* **24**, 52-56.
RAO, S. & HOUSKA, C. R. (1986*a*). *Acta Cryst.* A**42**, 6-13.
RAO, S. & HOUSKA, C. R. (1986*b*). *Acta Cryst.* A**42**, 14-19.
WARREN, B. E. (1959). *Prog. Met. Phys.* Vol. VIII.
WILKENS. M. (1970). *Theoretical Aspects of Kinematical X-ray Diffraction Profiles from Crystals Containing Dislocation Distributions.* In *Fundamental Aspects of Dislocation Theory*, edited by J. A. SIMMONS, R. DEWIT & R. BULLOUGH. *Natl Bur. Stand. (U.S.) Spec. Publ.* No. 317, p. 11.

*Acta Cryst.* (1988). A**44**, 1028-1035

# The Identification of $Sb_5O_7I$ Polytypes from Optical Properties in the Ferroic Phase

BY I. R. JAHN, W. ALTENBURGER AND W. PRANDL

*Institut für Kristallographie der Universität Tübingen, Charlottenstrasse* 33, *D*-7400 *Tübingen, Federal Republic of Germany*

AND V. KRÄMER

*Kristallographisches Institut der Universität Freiburg, Hebelstrasse* 25, *D*-7800 *Freiburg, Federal Republic of Germany*

(*Received* 4 *January* 1988; *accepted* 1 *June* 1988)

*Dedicated to Professor H. Dachs on the occasion of his 60th birthday*

## Abstract

The polytypic stacking sequences of $Sb_5O_7I$ (SOI) which are possible up to a ten-module period are derived together with their most probable space groups. It is found that the driving force of the reversible structural phase transition occurring in all polytypes is systematically modified by the polytypic degree of freedom. By defining only three interlayer interactions - each realized in a pure way by a simple polytype - the transition temperature $T_c$ of any stacking sequence can be predicted. The indicatrix orientation of SOI crystals depends on the proportion of + and − modules in a sequence. The extinction angle $\alpha$ is calculated on the basis of experimental data. The independent variables $T_c$ and $\alpha$ are used for the identification of six higher polytypes of $Sb_5O_7I$.

## 1. Introduction

The determination of polytypic structures from bulk physical properties alone is restricted by severe conditions. The polytypic degree of freedom should influence several properties of a compound in a different manner. Of course, the effects would have to be measurable with a high accuracy in order to detect the tiny differences between long stacking sequences. Large samples without stacking faults are needed. In a few cases optical studies have proved to be useful. In ZnS polytypes, for example, the number of hexagonal stackings per identity period could be derived from the birefringence (Brafman & Steinberger, 1966).

Among all the polytypic structures antimony(III) oxide iodide, $Sb_5O_7I$ (SOI), has a unique position (Nitsche, Krämer, Schuhmacher & Bussmann, 1977). Each modification undergoes a reversible structural phase transition which does not interfere with the polytypic degree of freedom itself. The polytypism, however, influences the properties of SOI fundamentally. This is indicated by the individual transition temperatures ($438 \leq T_c \leq 481$ K) of the eight polytypes distinguished so far and, more clearly, by the fact that some of them show pure ferroelasticity whereas others combine ferroelastic and ferroelectric behaviour in the low-symmetric phase. In principle, any ferroic property of SOI could be checked to see whether it contributes to the identification of the higher polytypes. The studies performed until now do not suffice for such an analysis.

This work was stimulated by the observation that the polytypic modifications of SOI differ in their crystal optics (Nitsche, Krämer, Schuhmacher & Bussmann, 1977). We analyse the differences in detail. It is demonstrated that $Sb_5O_7I$ offers for the first time the chance to attack successfully the identification problem of a complex polytypic structure simply by measuring bulk physical properties of the system. We first describe the structure of SOI and discuss suitable

0108-7673/88/061028-08$03.00 

symbolisms for the description of stacking sequences. A systematic treatment of all possible polytypes up to ten modules is presented in § 3. Then we analyse how the transition temperature $T_c$ (§ 4) and the extinction position $\alpha$ of a crystal (§ 5) are related to the module sequences. The different laws obtained for $T_c$ and $\alpha$ will be applied in § 6.

## 2. Structure and notation

Single crystals of SOI have been grown by a vacuum sublimation technique (Krämer, Nitsche & Schuhmacher, 1974). The (pseudo-) hexagonal prisms or pyramids are transparent and colourless, and are perfectly cleavable parallel to the basal plane. At 300 K, all polytypes are ferroelastic, while the noncentrosymmetric modifications additionally show ferroelectric behaviour. According to the hexagonal symmetry of the prototypic phase, three stable orientation states or domains exist in the ferroic phase, differing from each other by a rotation of ±120° around the stacking axis. They can be switched by stress and/or an electric field applied parallel to the basal plane. Based on the room-temperature structures of the two simplest and most abundant SOI polytypes (Krämer, 1975, 1978), the construction principle of the polytypic modifications has been derived by Nitsche, Krämer, Schuhmacher & Bussmann (1977). Very recently, the first high-temperature structure of the SOI polytypes was solved (Altenburger, Hiller & Jahn, 1988). We describe the polytypism in the high-symmetric state.

SOI consists of $\{Sb_2[Sb_3O_7]\}^+_\infty$ layers with symmetry $\bar{6}$ stacked one upon another and connected by an intermediate iodine layer. One Sb–O layer together with one adjacent I layer will be termed a module of SOI. Fig. 1(*a*) shows the projection of a module onto the basal plane. Successive modules are rotated by $n\times60°$ (with $n$ odd) against each other around the $\bar{6}$ axis on which the iodine atoms are located.

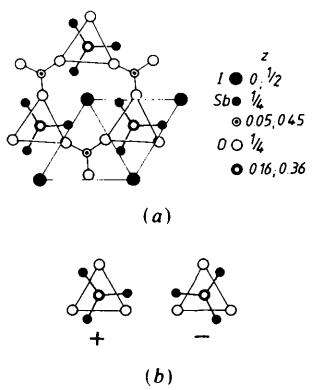


Fig. 1. (*a*) Module (+) of $Sb_5O_7I$ projected onto the basal plane. The Sb triangles (full circles) are in the mirror plane of the Sb–O layer. (*b*) $[Sb_3O_7]^{5-}$ building units with the Sb triangle in the + and − position, respectively.

The polytypism is caused by the fact that the Sb triangle of the $[Sb_3O_7]^{5-}$ building unit can occupy two equivalent positions relative to the oxygen prism (Fig. 1*b*). Within one layer, however, only one orientation is realized. We characterize these modules by a + and − sign, respectively. Two basic structures result: a centrosymmetric one containing a pair of identical modules, written as |++| or |−−|, and a noncentrosymmetric structure with two different modules, |+−| or |−+|. The higher polytypes are combinations of these basic units. The basic stackings differ in the Sb coordination polyhedron of the I atom as shown in Fig. 2. In |++|, the idealized Sb arrangement forms a cuboctahedron corresponding to the coordination polyhedron of a cubic close packing of spheres (*k* configuration). The 'anti-cuboctahedron' (Nitsche, Krämer, Schuhmacher & Bussmann, 1977) of type |+−| corresponds to hexagonal close packing (*h* configuration). The site symmetry of the I atom in |++| and |+−| is $\bar{3}$ and 32, respectively (Altenburger, Hiller & Jahn, 1988).

In polytypic structures whose lattices are built up from non-translationally equivalent layer packets, special notations are often very convenient. For SOI, several systems have been suggested by Nitsche, Krämer, Schuhmacher & Bussmann (1977). Adopted so far is a modified Ramsdell (1947) notation which additionally indicates the important information about whether a polytype is centrosymmetric (*C*) or not (*A*). The hexagonal basic types |++| and |+−| are indicated as 2*HC*- and 2*HA*-SOI, respectively. This

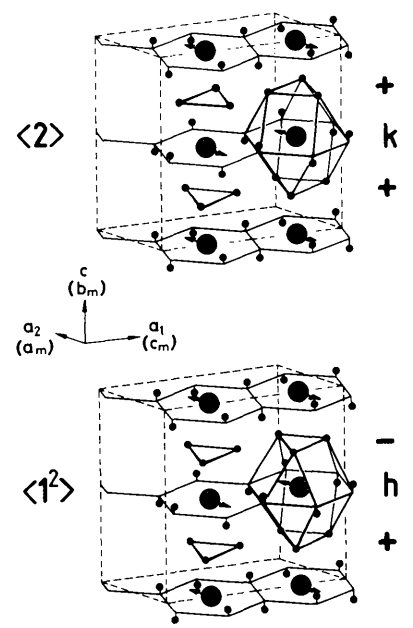


Fig. 2. Perspective view of the Sb–I framework of the basic structures |++| and |+−|. The *k*- and *h*-type Sb coordination polyhedra are shown. The arrows indicate the antiferro-displacement of the iodine atoms in the ferroic phase as well as the unit-cell doubling.

Table 1. *Polytypes of* $Sb_5O_7I$ *up to* $N = 8$ *and their properties*

| $N$ | Zhdanov sequence* | Ferroic phase: Ramsdell modified† | Ferroic phase: Space group | Paraphase: Space group | Transition temperature: $T_c$(K) (exp.) | Transition temperature: $T_c$(K) (calc.) | Extinction angle: $\alpha$(°) (exp.) | Extinction angle: $\alpha$(°) (calc.) |
|---|---|---|---|---|---|---|---|---|
| 2 | ⟨2⟩ | 2*MC* | $P2_1/c$ | $P6_3/m$ | 480·9 | — | 13·0 (2) | — |
| | $\langle 1^2\rangle$ | 2*MA* | *Pc* | $P\bar{6}2c$ | 437·6 | — | 0·0 (2) | — |
| 4 | $\langle 2^2\rangle$ | 4*TcC* | $P\bar{1}$ | $P\bar{3}c1$ | 455·1 | — | 0·0 (2) | 0 |
| | ⟨31⟩ | 4*MA* | *Pc* | $P\bar{6}$ | 458·8 | 457·2 | 8·1 (3) | 7·8 |
| 6 | ⟨42⟩ | 6*TcC* | $P\bar{1}$ | $P\bar{3}$ | 464·4 | 463·7 | 5·5 (3) | 5·5 |
| | $\langle 21\rangle_2$ | 6*MC* | $P2_1/c$ | $P6_3/m$ | — | 449·3 | — | 5·5 |
| | ⟨51⟩ | $6MA_1$ | *Pc* | $P\bar{6}$ | — | 465·1 | — | 9·8 |
| | $\langle 3^2\rangle$ | $6MA_2$ | *Pc* | $P\bar{6}2c$ | 463·5 | 463·7 | 0·0 (3) | 0 |
| | $\langle 31^3\rangle$ | $6MA_3$ | *Pc* | $P\bar{6}$ | — | 450·7 | — | 5·5 |
| | $\langle 1^221\rangle$, $\langle 121^3\rangle$ ‡ | 6*TcA* | *P*1 | *P*321 | 448·8 | 449·3 | 0·0 (3) | 0 |
| 8 | ⟨62⟩ | $8TcC_1$ | $P\bar{1}$ | $P\bar{3}$ | 466·4 | 468·0 | 7·8 (3) | 7·8 |
| | $\langle 4^2\rangle$ | $8TcC_2$ | $P\bar{1}$ | $P\bar{3}c1$ | 468·1 | 468·0 | 0·0 (3) | 0 |
| | ⟨4121⟩ | $8TcC_3$ | $P\bar{1}$ | $P\bar{3}$ | — | 457·2 | — | 7·8 |
| | $\langle 211\rangle_2$ | $8TcC_4$ | $P\bar{1}$ | $P\bar{3}c1$ | — | 446·4 | — | 0 |
| | ⟨71⟩ | $8MA_1$ | *Pc* | $P\bar{6}$ | — | 469·0 | — | 10·7 |
| | ⟨53⟩ | $8MA_2$ | *Pc* | $P\bar{6}$ | 467·7 | 468·0 | 3·9 (3) | 4·3 |
| | $\langle 51^3\rangle$ | $8MA_3$ | *Pc* | $P\bar{6}$ | — | 458·2 | — | 7·8 |
| | $\langle 1^223\rangle$, $\langle 321^3\rangle$ ‡ | $8TcA_1$ | *P*1 | *P*321 | — | 457·2 | — | 4·3 |
| | $\langle 231^3\rangle$, $\langle 1^332\rangle$ ‡ | $8TcA_2$ | *P*1 | *P*3 | — | 457·2 | — | 0 |
| | $\langle 2^31^2\rangle$, $\langle 1^22^3\rangle$ ‡ | $8TcA_3$ | *P*1 | *P*3 | — | 456·1 | — | 4·3 |
| | ⟨3212⟩ | $8MA_4$ | *Pc* | $P\bar{6}$ | — | 456·1 | — | 0 |
| | $\langle 31^5\rangle$ | $8MA_5$ | *Pc* | $P\bar{6}$ | — | 447·4 | — | 4·3 |
| | $\langle 1^421^2\rangle$ | $8MA_6$ | *Pc* | $P\bar{6}$ | — | 446·4 | — | 4·3 |
| | $\langle 1^521\rangle$, $\langle 121^5\rangle$ ‡ | $8TcA_4$ | *P*1 | *P*3 | — | 446·4 | — | 0 |

* The first character gives the number of + modules, $\nu_+$.

† The second letter (*C* or *A*) indicates whether a polytype structure is centrosymmetric or not (Nitsche, Krämer, Schuhmacher & Bussmann, 1977).

‡ Homometric pair. The nomenclature used in this paper deviates slightly from IUCr recommendations. It has, however, the advantage that homometric variants are uniquely labelled.

notation does not disclose the relationship between the layers; moreover, the symbol changes at the phase transition.

For the specification of the exact stacking sequence of modules we suggest the (+, −) symbolism introduced above. It represents a simplification of Nitsche's ($\overset{+}{A}$, $\overset{-}{A}$, $\overset{+}{B}$, $\overset{-}{B}$) notation. We note that our system differs from Hägg's (1943) symbolism which indicates two alternative positions of a building layer relative to the preceding one. As usual, we simplify the sequence of characters + and − to the shorthand form of Zhdanov's (1945) symbolism by indicating the numbers $\nu_+$ and $\nu_-$ of the consecutive characters + and −, respectively. Homometric polytypes of SOI can only be distinguished if the symbol starts with the same character for all polytypes. We choose $\nu_+$ as the first number in Zhdanov's sequence. The two-module polytypes |++| and |+−| are given by the symbols $\langle 20\rangle \equiv \langle 2\rangle$ and $\langle 11\rangle \equiv \langle 1^2\rangle$, respectively. It should be noted that Jagodzinski's (1949) (*h*, *k*) symbolism could also be used. In our discussion of the interlayer interactions (§ 4), the Sb–I coordination geometry plays an essential role.

The room-temperature structures of ⟨2⟩ and $\langle 1^2\rangle$, 2*MC*-SOI (Krämer, 1975) and 2*MA*-SOI (Krämer, 1978), as well as that of the four-module type ⟨31⟩, 4*MA*-SOI (Bussmann, 1978), clearly indicate that the characteristic feature of the ferroic phase is the antiferro-displacement of neighbouring iodine atoms. The displacement direction is nearly parallel to one of the hexagonal *a* axes (which becomes the monoclinic *a* axis). The unit cell is doubled along one of the other hexagonal *a* axes (monoclinic *c* axis). In Fig. 2, iodine displacements and unit cells of 2*MC*- and 2*MA*-SOI are schematically shown. The phase transition destroys the threefold axis, and the mirror plane within the Sb–O layer is reduced to a glide plane along **c**. At $T_c$, the space group of ⟨2⟩ transforms from $P6_3/m$ (Krämer, Nitsche & Schuhmacher, 1974) into $P2_1/c$ (Krämer, 1975). The sequence of $\langle 1^2\rangle$,

$P\bar{6}2c$ (Altenburger, Hiller & Jahn, 1988) → $Pc$ (Krämer, 1978) does not follow a direct group–maximal subgroup relation.

It is important to note that a parent phase common to all polytypic modifications of SOI has not been found up to the decomposition temperature of about 820 K. A change in the polytypic state could only arise if the Sb atoms of the $[Sb_3O_7]^{5-}$ unit interchange their positions + and − within the Sb-O layers.

### 3. Stacking sequences of $Sb_5O_7I$ and their space groups

For the identification procedure we need all stacking sequences which are possible for a given number of modules per repeat unit. The highest polytypes known for SOI comprise eight modules. Therefore, the combinatorial analysis will be restricted to $N = 10$. For a given $N$ (even), all combinations of the basic units $|{+}{+}|$ and $|{+}{-}|$ as well as of their equivalents $|{-}{-}|$ and $|{-}{+}|$ are generated. The permutations are then analysed according to whether they can be reduced to already known sequences, either of the same $N$ (simply by a suitable choice of the identity period along the stacking axis) or of a smaller stacking height. The number of different sequences diminishes by a factor of two because the sequence of a crystal does not change if the crystal is rotated. A 180° rotation around an axis parallel to the layers inverts the stacking sequence and, at the same time, + changes into − and *vice versa*. For the sake of clarity, the setting of all polytypes is chosen in such a manner that $n_+ \geq n_-$, with $n_+$ and $n_-$ being the total number of + and − modules per repeat. The possible polytypic sequences up to $N = 8$ are given in Table 1. Besides the two types for $N = 4$ we find seven for $N = 6$ [as against the four stated by Nitsche, Krämer, Schuhmacher & Bussmann (1977)] and 18 modifications for $N = 8$. For $N = 10$, 60 sequences are derived, nine of which are centrosymmetric. They cannot be listed here; however, their properties determined in this work are included in Fig. 7.

Using the known structural data one is able to predict the probable space groups for both phases of the polytypes. We start from the high-temperature point symmetry $\bar{6}$ of the Sb-O layer. In constructing a polytype, the mirror operation is only maintained if it fits into the stacking sequence, too. Whether this is the case can easily be seen from the (+, −) sequence. If the sequence of characters on both sides of the module in question is symmetrical to the module itself, then $m$ may exist. As an example, for polytype ⟨31⟩ the modules containing a mirror plane are marked by the dots $|\dot{+}\dot{+}{+}\dot{-}|$. The high-temperature space group of a modification with a mirror plane is $P\bar{6}$ and $P3$ without. In the case of an additional centre of symmetry, the space groups will be $P6_3/m$ and $P\bar{3}$, respectively. Whether a polytype is centrosymmetric or not can be read off again from the (+, −) symbolism simply by looking for symbolic mirror symmetry between the characters. If these mirrors are present, as shown for type ⟨$2^2$⟩ by the dots in the sequence $-|{+}\cdot{+}{-}\cdot{-}|{+}$, the polytype is centrosymmetric. Below $T_c$ the noncentrosymmetric space groups are $Pc$ and $P1$, and the centrosymmetric ones $P2_1/c$ and $P\bar{1}$, respectively. The probable high- and low-temperature space groups obtained for the stackings up to $N = 8$ are listed in Table 1. The sequences for a given $N$ are grouped in centrosymmetric and noncentrosymmetric structures, and within each category they are arranged according to their $T_c$ values as determined in the next section.

### 4. Transition temperature

Nitsche, Krämer, Schuhmacher & Bussmann (1977) observed the $T_c$ spread of the SOI polytypes and used it for the discrimination. An explanation was not given. In this section we relate polytype structure and transition temperature. We suppose that the mechanisms of the structural phase transition are essentially the same in all polytypes. The similarity shows up in the temperature dependence of the in-plane birefringence, $\Delta n_{010}(T)$, given in Fig. 3. The results for three polytypes are omitted for clarity. In all cases, the phase transition is very weakly of first order. A detailed discussion of the order-parameter behaviour and the influence of the iodine site symmetry will be given separately (Altenburger, Bosch, Jahn & Krämer, 1988). A short account has been presented earlier (Jahn, Altenburger, Bosch & Krämer, 1983). The basic polytypes ⟨2⟩ and ⟨$1^2$⟩ reveal the extreme $T_c$ values, $T_c(\langle 2\rangle) = 480{\cdot}9$ and $T_c(\langle 1^2\rangle) = 437{\cdot}6$ K; those of the identified four-module types ⟨31⟩ (4*MA*) and ⟨$2^2$⟩ (4*TcC*; Nitsche, Krämer, Schuhmacher & Bussmann, 1977) are slightly less than the mean value of 459 K, $T_c(\langle 31\rangle) = 458{\cdot}5$ and $T_c(\langle 2^2\rangle) = 455{\cdot}1$ K. The relative accuracy in determining $T_c$ is about 0·2 K.

For a phenomenological description of the phase transition, we introduce an interaction which can be

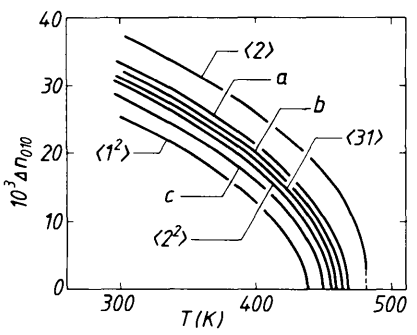


Fig. 3. Temperature-dependent birefringence $\Delta n_{010}$ of seven SOI polytypes in the ferroic phase (Altenburger, Bosch, Jahn & Krämer, 1988). The sequences of *a*, *b*, *c* as determined in § 6 are ⟨$4^2$⟩, ⟨$3^2$⟩ and ⟨$1^3$21⟩/⟨12$1^3$⟩, respectively.

adapted to the polytypic degree of freedom. We propose as the driving force an interaction between successive iodine layers whereby the intermediate Sb-O framework is strongly involved. The antiferrodisplacement of the iodine atoms is triggered by an antiphase tilt motion of the $[Sb_3O_5]^{5-}$ units as shown in Fig. 4. Owing to the different Sb coordination geometries we may distinguish between three types of I-I interlayer interactions.

Type *H*: The iodine atoms of both layers are in *h* configuration as realized in polytype $\langle 1^2 \rangle$.

Type *K*: The *kk* configuration arises in polytype $\langle 2 \rangle$.

Type *M*: Adjacent iodine layers differ in their Sb configuration. This mixed type can be realized only in combinations of the basic types $\langle 1^2 \rangle$ and $\langle 2 \rangle$.

The energy per layer of these I-I interactions is denoted by $J_H$, $J_K$ and $J_M$, respectively. Each polytype may also be represented by the sequence of interactions.

The I-I interactions are expected to show up in characteristic differences of the atomic displacements occurring at $T_c$. Therefore, the room-temperature structures of $\langle 2 \rangle$ (2*MC*), $\langle 1^2 \rangle$ (2*MA*) and $\langle 31 \rangle$ (4*MA*) are analysed with respect to the atomic displacements along the stacking axis. We confine ourselves to the I atoms and the Sb triangles at top and bottom of the Sb cages. These atoms occupy special *z* positions (0, $\frac{1}{8}$, $\frac{1}{4}$, ... *etc.*) in the non-ferroic phase. Their displacements multiplied by a factor of ten are given in Fig. 5. The polytypes $\langle 2 \rangle$ and $\langle 1^2 \rangle$ differ fundamentally. In the *kk* configuration, all atoms show in-phase displacements along [010]. In configuration *hh*, on the other hand, the Sb triangles of adjacent layers are displaced in antiphase and, consequently, the iodine atoms do not move at all. From this discussion we arrive at the conclusion that in the mixed type *hk* only the iodine atoms of the *k* layer should move along the stacking axis, whereas the *h* layer should be stable at $T_c$. Polytype $\langle 31 \rangle$ contains the three configurations (Fig. 5). The predicted *hk* pattern is nearly realized. Some of the iodine atoms show very small deviations from the 'ideal' scheme which may be indicative of longer-ranged interactions present in $\langle 31 \rangle$. We point out that the ideal *hk* pattern should be realized in polytype $\langle 2^2 \rangle$. Unfortunately, the room-temperature structure of this type has not been determined. We suggest the pattern given in Fig. 5.

The experimental transition temperature of a system is related to the interaction energy *J* driving the phase transition. Tentatively we write

$$k_B T_c \propto J \quad (k_B = \text{Boltzmann constant})$$

and we assume that the same proportionality factor holds for all stacking sequences of the SOI polytypes. Then the different interaction energies may be expressed by the experimental $T_c$ values of the three pure types

$$J_K / T_c(\langle 2 \rangle) = J_H / T_c(\langle 1^2 \rangle) = J_M / T_c(\langle 2^2 \rangle).$$

For a strict nearest-neighbour interaction, the transition temperature of any stacking sequence follows from the mean value of the I-I interactions $J_H$, $J_K$, $J_M$ contained in a stacking period,

$$T_c^c = [n_K T_c(\langle 2 \rangle) + n_H T_c(\langle 1^2 \rangle) + n_M T_c(\langle 2^2 \rangle)] / N, \quad (1)$$

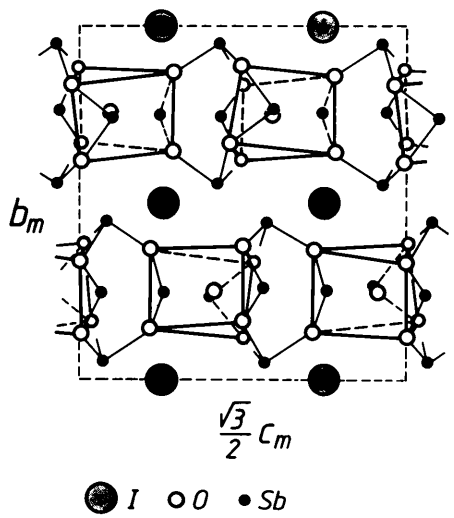


Fig. 4. Antiphase tilting of the $[Sb_3O_7]^{5-}$ unit in the ferroic phase of polytype $\langle 2 \rangle$ (view along the monoclinic *a* axis).

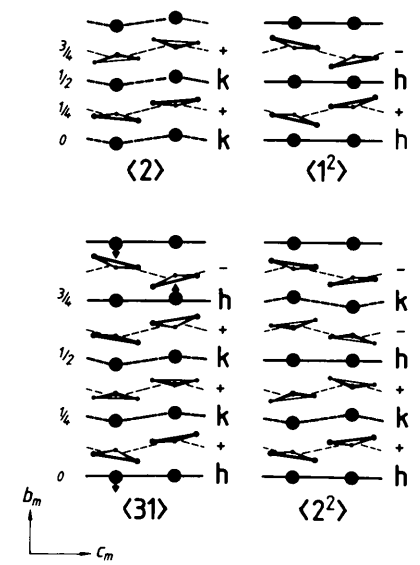


Fig. 5. Experimental room-temperature displacements (×10) of the I atoms and of the Sb triangles along the stacking axis. In polytype $\langle 31 \rangle$, the iodine shifts marked by arrows indicate the presence of longer-range interactions. The pattern of polytype $\langle 2^2 \rangle$ has been constructed on the basis of the experimental data of $\langle 2 \rangle$, $\langle 1^2 \rangle$ and $\langle 31 \rangle$.

where $n_K$, $n_H$, $n_M$ denote the number of the corresponding I-I interlayer interactions present in the $N$-module polytype.

As a first test, the transition temperature of polytype $\langle 31\rangle$ with $n_K = n_H = 1$, $n_M = 2$ is calculated. The result, $T_c^c(\langle 31\rangle) = 457{\cdot}2$ (2) K, has to be compared with the experiment. The quite large difference, $\Delta T_c(\langle 31\rangle) = T_c^c(\langle 31\rangle) - T_c(\langle 31\rangle) = -1{\cdot}3$ (4) K, seems to question the validity of the model. However, the agreement obtained in § 6 for the six- and eight-layer polytypes is convincing. The displacement pattern of $\langle 31\rangle$ (Fig. 5) and the sign of $\Delta T_c(\langle 31\rangle)$ both agree in that the interaction of the sequence *hk-kk-kh* is stronger than taken into account simply by $J_K + 2J_M$. Therefore, $\Delta T_c$ ($\langle 31\rangle$) quantifies the influence of longer-ranged interactions. The calculated transition temperatures of all polytypes up to $N = 8$ are listed in Table 1. In addition, Fig. 7 shows the data for $N = 10$.

It should be mentioned that the three polytypes $\langle 1^2\rangle$, $\langle 2\rangle$, $\langle 2^2\rangle$ representing the basic interactions $J_H$, $J_K$, $J_M$ provide the ground states in the axial next-nearest-neighbour Ising (ANNNI) model (Price & Yeomans, 1984): $\langle 2\rangle$ and $\langle 1^2\rangle$ for the interactions between adjacent layers (NN) with $J_1 > 0$ and $J_1 < 0$, respectively, and $\langle 2^2\rangle$ for a dominating NNN interaction with negative sign ($|J_1|$ small, $J_2 < 0$). This model is used to describe the energetics of polytypic systems. The interactions defined in our model are restricted to the structural phase transition where the polytypic degree of freedom is not changed.

## 5. Orientation of the indicatrix

A new phenomenon arises in $Sb_5O_7I$. The optical index ellipsoid rotates stepwise when the chemically identical modules are suitably stacked. Therefore, the polytypes can be characterized by their extinction angle (Nitsche, Krämer, Schuhmacher & Bussmann, 1977).

At room temperature, the SOI single crystals are optically biaxial. The indicatrix is free to rotate around the stacking axis. In polytype $\langle 1^2\rangle$, shape and position for a wavelength of 6328 Å are given by $n_\alpha = 2{\cdot}240$, $n_\beta = 2{\cdot}267$ and $n_\gamma = 2{\cdot}295$ with $n_\alpha$ parallel to the $b$ axis and $n_\beta$ practically parallel to **a** (Wischer, 1978). In accordance with Nitsche, Krämer, Schuhmacher & Bussmann (1977) we define as the extinction angle $\alpha$ of as-grown SOI single crystals the angle between the position of $n_\beta$ and those edges of the (pseudohexagonal) basal plane which are parallel to the monoclinic $a$ axis. For our study ten modifications were available, the eight types studied earlier as well as two new eight-module polytypes isolated since. Their stacking height was determined by X-ray powder diffraction. Under a polarizing microscope with phase-modulation technique (Modine, Major & Sonder, 1975) the extinction direction of a sample can be determined with an accuracy of better than 0·05°. In the case of SOI, the often non-ideal edges of the crystals caused a maximum uncertainty of $\delta\alpha \simeq 0{\cdot}3°$. The measurements were performed for a wavelength of 6328 Å (HeNe laser) at 300 K. No temperature dependence of $\alpha$ was observed.

The polytypes can be arranged into two distinct groups: there are five examples with $\alpha \simeq 0$ (straight extinction); the extinction of the others is oblique, with angles ranging between 4 and 13°. From the value of the identified polytypes, 0 for $\langle 1^2\rangle$ and $\langle 2^2\rangle$, 13° for $\langle 2\rangle$ and 8·1° for $\langle 31\rangle$, one immediately concludes that the rule for $\alpha$ differs fundamentally from that for $T_c$. It is not the stacking sequence which determines the indicatrix orientation but merely the proportion of + and − modules per repeat. This is shown in Fig. 6 where we use the linear scale $(n_+ - n_-)/N \equiv w$. We suppose a monotonic $\alpha(w)$ dependence for the modifications identified. Then the extinction angles of 5·5 and 3·9° which are found in a six- and an eight-module polytype fit in very well with possible weights $w$ of 2/6 and 2/8, respectively. $\alpha(w)$ is not a linear function in the full range of $w$. However, an approximate proportionality seems to hold in the range $0 \le w \le 1/2$. Unfortunately, no data are available for compositions $w < 0{\cdot}2$ and $w > 0{\cdot}5$, where polytypes with ten and more modules per repeat would be needed.

We propose as the essential principle of the interpretation the superposition of the dielectric tensors of the individual modules. The question arises whether the indicatrix position of a higher SOI polytype could be quantitatively reproduced by a simple model. We assume that the optical properties of the

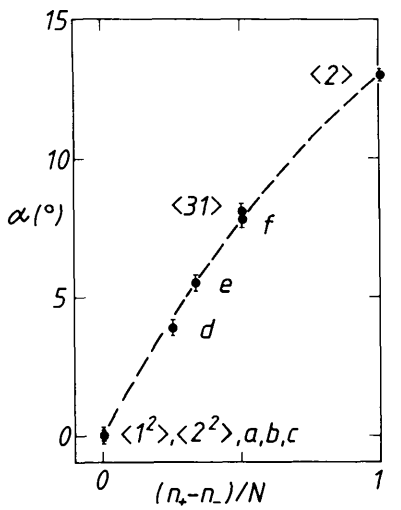


Fig. 6. Extinction angle $\alpha$ of the SOI polytypes as a function of the proportion of + and − modules. The letters denote modifications identified in § 6 of this paper: (*a*) $\langle 4^2\rangle$, (*b*) $\langle 3^2\rangle$, (*c*) $\langle 1^3 21\rangle/\langle 121^3\rangle$, (*d*) $\langle 53\rangle$, (*e*) $\langle 42\rangle$, (*f*) $\langle 62\rangle$. The dashed line is calculated from equation (3).

basic units can be described by the dielectric tensors of the polytypes $\langle 2\rangle$ and $\langle 1^2\rangle$, and we perform a linear superposition according to the weight $w$ of a polytype. Our simplification ignores the individual interference effects of the different stacking sequences which would be taken into account by a microscopic theory of the propagation of light in the crystal.

We consider crystal plates of the polytypes $\langle 2\rangle$ and $\langle 1^2\rangle$ for the case of normally incident light. Their dielectric tensors with axes of reference parallel to the principal axes are written by

$$\boldsymbol{\varepsilon}(j)=\begin{pmatrix}\varepsilon_1(j) & 0 & 0\\ 0 & \varepsilon_2(j) & 0\\ 0 & 0 & \varepsilon_1(j)-\Delta(j)\end{pmatrix}$$

with $j=1$ for type $\langle 1^2\rangle$ and 2 for $\langle 2\rangle$. The in-plane birefringence at room temperature is approximated by

$$\Delta n^{(j)}=\Delta(j)/\{2[\varepsilon_1(j)]^{1/2}\}. \qquad (2)$$

The tensor of type $\langle 1^2\rangle$ is adopted for the basic unit $|+-|$, $\boldsymbol{\varepsilon}^{+-}\equiv\boldsymbol{\varepsilon}(1)$. The first principal axis of $\boldsymbol{\varepsilon}^{+-}$ is parallel to the $a$ axis. According to the experimental extinction of type $\langle 2\rangle$, the angle between the first principal axis of tensor $\boldsymbol{\varepsilon}(2)$ and the $a$ axis is $\alpha_2=13°$. For the intended superposition of $\boldsymbol{\varepsilon}^{+-}$ and $\boldsymbol{\varepsilon}^{++}$, $\boldsymbol{\varepsilon}(2)$ has to be transformed,

$$\boldsymbol{\varepsilon}^{++}=\mathbf{R}^{-1}(\alpha_2)\boldsymbol{\varepsilon}(2)\mathbf{R}(\alpha_2),$$

$$\mathbf{R}(\alpha_2)=\begin{pmatrix}\cos\alpha_2 & 0 & -\sin\alpha_2\\ 0 & 1 & 0\\ \sin\alpha_2 & 0 & \cos\alpha_2\end{pmatrix}.$$

Now, we superpose both units weighted by $w^{++}\equiv w=(n_+-n_-)/N$ and $w^{+-}=1-w$, respectively. The resulting dielectric tensor for a given proportion of $n_+$ and $n_-$ is

$$\boldsymbol{\varepsilon}(w)=w\boldsymbol{\varepsilon}^{++}+(1-w)\boldsymbol{\varepsilon}^{+-}.$$

The extinction angle $\alpha(w)$ is obtained by diagonalization of $\boldsymbol{\varepsilon}(w)$ with $\mathbf{R}[\alpha(w)]$,

$$\tan 2\alpha(w)=\sin 2\alpha_2/\{[\Delta(1)/\Delta(2)](1/w-1)+\cos 2\alpha_2\}. \qquad (3)$$

The $w$-dependent birefringence can also be derived,

$$\Delta(w)=[(1-w)^2\Delta^2(1)+w^2\Delta^2(2)+2w(1-w)\Delta(1)\Delta(2)\cos 2\alpha_2]^{1/2}. \qquad (4)$$

This relation, however, gives only a crude approximation; owing to the phase transition, the birefringence of the polytypes depends on the stacking sequence itself.

The refractive indices of type $\langle 2\rangle$ have not been measured so far. By assuming $\varepsilon_1(1)=\varepsilon_1(2)$ and using the measured 300 K birefringence of $\langle 2\rangle$ and $\langle 1^2\rangle$ (Fig. 3) in (2), the ratio $\Delta(1)/\Delta(2)\simeq 0{\cdot}68$. The calculated $\alpha(w)$ is given in Fig. 6. Considering the strong simplifications made in our model, we find the agreement with the experimental extinction angles to be surprisingly good. We are able to predict the indicatrix position for all polytypic modifications of $Sb_5O_7I$. The angles for the $N\leq 8$ polytypes are listed in Table 1, those of $N=10$ are given in Fig. 7.

We note finally that the straight extinction is atypical for monoclinic and triclinic symmetry. It has been shown for polytype $\langle 1^2\rangle$ that the positions of all atoms in space group *Pc* do not vary significantly from those in the orthorhombic group *Pnn*2 (Krämer, 1978). However, piezoelectric measurements indicate that the glide plane parallel to the stacking axis is not strictly realized. Obviously, the crystal optics cannot contribute to this question. Straight extinction is found in all polytypes with $n_+=n_-$, even in types where the glide plane is clearly excluded by the construction principle of the structure, as in polytype $\langle 2^2\rangle$, for example.

## 6. Determination of stacking sequences

In this section, we demonstrate the application of our model. Any polytypic modification of SOI can be characterized by a set of properties, $(\alpha|T_c)$, which either allows the identification of a polytype directly or, at least, reduces the number of stacking sequences in question appreciably. Of course, knowing the stacking height from an X-ray experiment would be very helpful. In Fig. 7, the field of possible $(\alpha|T_c)$ couples is shown for sequences up to $N=10$.

We analyse six polytypes with $N=6$ and 8. Their Ramsdell symbols introduced by Nitsche, Krämer, Schuhmacher & Bussmann (1977) will be retained if possible. Polytype $6TcC$ is characterized by

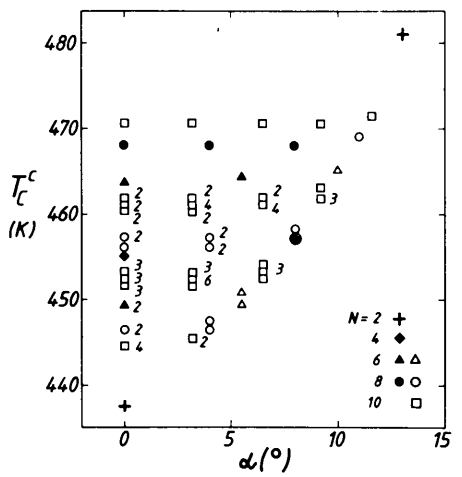


Fig. 7. Calculated transition temperature *versus* calculated extinction angle for the polytypes up to $N=10$. The numbers give the ambiguity of the corresponding $(\alpha|T_c^c)$. Crosses and full symbols belong to identified types.

($\alpha = 5{\cdot}5°$ | $T_c = 464{\cdot}4$ K). Table 1 offers only one sequence for this set, namely polytype ⟨42⟩. The difference $\Delta T_c(\langle 42\rangle) = -0{\cdot}7$ (4) K, presumably due to longer-ranged interlayer interactions, is about half of the value found for ⟨31⟩.

Contradictions arise for the polytypes '$6MA_1$' and '$8TcC_1$' in Nitsche's work having the data sets (3·9°|467·7 K) and (0|463·5 K), respectively. In the case of '$6MA_1$', neither $\alpha$ nor $T_c$ value can be brought into line with $N = 6$ in Table 1. Instead, the data agree excellently with (4·3°|468·0 K) as calculated for the eight-layer polytype ⟨53⟩. On the other hand, the data of polytype '$8TcC_1$' do not fit into the $N = 8$ group. Its $T_c$ deviates by more than 4 K from the $\alpha = 0$ candidates in question. However, the data would be in best agreement with the six-layer sequence $\langle 3^2\rangle$. We therefore believe that some of the data of these two polytypes have been interchanged in the work by Nitsche, Krämer, Schuhmacher & Bussmann (1977). Of course, there remains the problem that $\langle 3^2\rangle$ is noncentrosymmetric whereas type '$8TcC_1$' apparently did not show piezoelectric/ferroelectric properties.

Two possibilities exist for the polytype with (0°|448·8 K), namely the sequences $\langle 1^321\rangle$ and $\langle 121^3\rangle$. These types are homometric and cannot be discriminated from $\alpha$ and $T_c$. Their ferroic phase is expected to be triclinic with the Ramsdell symbol $6TcA$ (instead of Nitsche's '$6MA_2$'). The identification of the two remaining $N = 8$ sequences is straightforward, too. Full agreement is obtained for the polytype $\langle 4^2\rangle$ ($8TcC_2$). Finally, the set (7·8°|466·4 K) can only be correlated with the sequence ⟨62⟩ (our Ramsdell symbol $8TcC_1$). Unfortunately, only one crystal of this rare species was available. The positive $\Delta T_c$ value of 1·6 K seems to point to the existence of stacking faults in this crystal.

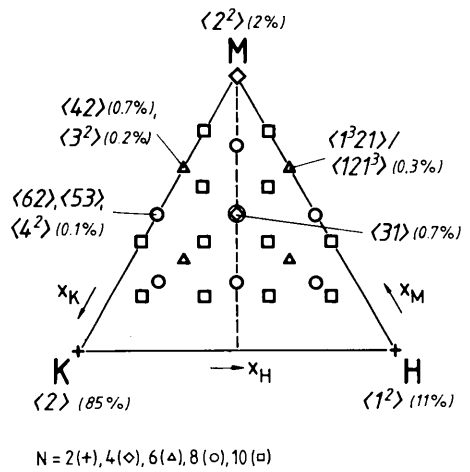


Fig. 8. The possible 'concentrations' of the I-I interaction types $H$, $K$ and $M$ in the SOI polytypes up to $N = 10$.

Based on the interactions $H$, $K$ and $M$ the polytypes of $Sb_5O_7I$ can be conceived as isolated points in a ternary diagram with the three types $\langle 1^2\rangle$, ⟨2⟩ and $\langle 2^2\rangle$ as the pure end members. Fig. 8 shows the concentration triangle with all possible mixtures up to $N = 10$. The allowed concentrations are given by $x_{K,H} = n_{K,H}/N$ with $n_{K,H} = 0, 1, 2, \ldots, N$ and $x_M = n_M/N$; $n_M = 0, 2, \ldots, N$, respectively. The case of $n_M = 0$ is realized only by the end members ⟨2⟩ and $\langle 1^2\rangle$ because any mixture of $H$ and $K$ leads to $n_M \neq 0$. The identified polytypes together with their relative abundances (Nitsche, Krämer, Schuhmacher & Bussmann, 1977) are also given in Fig. 8. We see that polytype ⟨31⟩ is the only ternary mixture. Depending on the highly abundant basic type ⟨2⟩ the mixtures of $K$ and $M$ are favoured. Except for the type $\langle 1^321\rangle/\langle 121^3\rangle$, all polytypes of $Sb_5O_7I$ found so far are of the simple type $\langle n_+ n_-\rangle$.

Financial support by the Deutsche Forschungsgemeinschaft is gratefully appreciated.

## References


ALTENBURGER, W., BOSCH, G., JAHN, I. R. & KRÄMER, V. (1988). In preparation.

ALTENBURGER, W., HILLER, W. & JAHN, I. R. (1988). *Z. Kristallogr.* **181**, 227-234.

BRAFMAN, O. & STEINBERGER, I. T. (1966). *Phys. Rev.* **143**, 501-505.

BUSSMANN, A. (1978). *Untersuchungen der ferroischen Eigenschaften der Polytypen des Antimon*(III)-*Oxid-Iodids* $Sb_4O_7I$. Dissertation, Univ. Freiburg, Federal Republic of Germany.

HÄGG, G. (1943). *Ark. Kem. Mineral. Geol.* **16B**, 1-6.

JAGODZINSKI, H. (1949). *Acta Cryst.* **2**, 201-207.

JAHN, I. R., ALTENBURGER, W., BOSCH, G. & KRÄMER, V. (1983). *Z. Kristallogr.* **162**, 118-120.

KRÄMER, V. (1975). *Acta Cryst.* **B31**, 234-237.

KRÄMER, V. (1978). *Acta Cryst.* **B34**, 2695-2698.

KRÄMER, V., NITSCHE, R. & SCHUHMACHER, M. (1974). *J. Cryst. Growth*, **24/25**, 179-182.

MODINE, F. A., MAJOR, R. W. & SONDER, E. (1975). *Appl. Opt.* **14**, 757-760.

NITSCHE, R., KRÄMER, V., SCHUHMACHER, M. & BUSSMANN, A. (1977). *J. Cryst. Growth*, **42**, 549-559.

PRICE, G. D. & YEOMANS, J. (1984). *Acta Cryst.* **B40**, 448-454.

RAMSDELL, L. S. (1947). *Am. Mineral.* **32**, 64-82.

WISCHER, J. (1978). *Optische Frequenzverdopplung und Untersuchung des strukturellen Phasenübergangs in* $2MA$-$Sb_5O_7I$. Diplomarbeit, Univ. Würzburg, Federal Republic of Germany.

ZHDANOV, G. S. (1945). *C.R. (Dokl.) Acad. Sci. URSS*, **48**, 40-43.